第 25 卷第 11 期
2009 年 11 月

无 机 化 学 学 报
CHINESE JOURNAL OF INORGANIC CHEMISTRY

Vol.25 No.11
2031~2035

$Sr_2Ta_2O_7$ 纳米片的水热合成及其高效光降解甲基橙溶液的性能研究

周 超 陈 刚* 张红杰 王 群
(哈尔滨工业大学化学系,哈尔滨 150001)

摘要: 采用水热法制备了 $Sr_2Ta_2O_7$ 纳米片,并通过 XRD、UV-Vis、SEM 和 TEM 等手段对其进行了表征。以降解甲基橙溶液为反应模型,研究了 $Sr_2Ta_2O_7$ 纳米片的光催化性能。光催化结果表明,水热法制备的 $Sr_2Ta_2O_7$ 纳米片具有更高的光催化降解效率,为固相法制备的块体 $Sr_2Ta_2O_7$ 样品的 2 倍。二者催化性能上差异主要是由于两种方法制备的样品具有不同的晶粒大小和比表面积造成的。

关键词: $Sr_2Ta_2O_7$; 纳米片; 光催化; 甲基橙
中图分类号: O614.23+2; O614.51+3 **文献标识码**: A **文章编号**: 1001-4861(2009)11-2031-05

Efficient Photocatalytic Degradation of Methyl Orange over Hydrothermally Synthesized $Sr_2Ta_2O_7$ Nanosheets

ZHOU Chao CHEN Gang* ZHANG Hong-Jie WANG Qun
(*Department of Chemistry, Harbin Institute of Technology, Harbin* 150001)

Abstract: $Sr_2Ta_2O_7$ nanosheets were prepared via a hydrothermal route and were characterized by XRD, UV-Vis absorption spectra, SEM and TEM. The photocatalytic activity of $Sr_2Ta_2O_7$ nanosheets was investigated using the degradation of methyl orange as a model reaction. Photocatalytic results show that the $Sr_2Ta_2O_7$ nanosheets exhibit higher degradation efficiency, 2 times higher than that of the bulk $Sr_2Ta_2O_7$ sample. The different photocatalytic performances are mainly ascribed to the difference in the crystal size and surface area.

Key words: $Sr_2Ta_2O_7$; nanosheets; photocatalytic; methyl orange

0 Introduction

Since the Hon da-Fujishima effect was reported using a TiO_2 semiconductor electrode, photocatalytic reactions of semiconductors, such as splitting of water and degradation of organic and inorganic pollutants, have been received great attention[1~6]. Although much work has been developed to exploit new photocatalysts under ultraviolet and visible light irradiation, the number of effective photocatalysts for degradation of the pollutant contaminates is still limited[7~12]. Therefore, it is urgent to develop a new type of photocatalyst with high photocatalytic activity. On the other hand, most of those photocatalysts are generally prepared by conventional solid-state reactions(SSR). Although significant progress has been made, such syntheses are limited by the problems commonly associated with solid state synthesis, including the difficulty in crystal growth, segregation of components, and uncertainty in stoichiometry, all potentially contributing to the compromised photocatalytic activity[13]. Considering the need to obtain pure and homogeneous crystalline

收稿日期:2009-07-14。收修改稿日期:2009-10-05。
国家自然科学基金(No.20871036)、哈尔滨市优秀学科带头人基金(No.2006RFXXG001)资助项目。
*通讯联系人。E-mail:gchen@hit.edu.cn,Tel:86-451-86413753
第一作者:周 超,男,27 岁,博士研究生;研究方向:光催化材料在能源和环境中的应用。

powders with high photocatalytic activity, an alternative synthesis procedure is required.

Hydrothermal synthesis as a well-known traditional wet chemical process has been widely used to synthesize advanced nanostructures because of its advantages [14 ~17]. It is believed that this method generates highly crystalline products with high purity, low aggregation, controlled size and morphology. Recently, hydrothermal synthesis has been widely employed to prepare nanosized crystallites with high purity and novel morphologies to enhance photocatalytic activity. Bao et al[18] reported that N-doped nanocrystal TiO_2 powders prepared via a hydrothermal reaction-thermolysis process showed higher photocatalytic activity for degradation of liquid reactive brilliant red X-3B under visible light irradiation. Fu et al[19] reported that nanosized Bi_2WO_6 sheets exhibited relatively high photochemical activity for the decomposition of rhodamine-B under visible light irradiation (λ >420 nm); ZnSe nanoflowers exhibited higher photocatalytic activity for the photodegradation of methylene blue and ethyl violet under UV light irradiation than the commercially available photocatalyst P25[20]; Dumbbell-like and rod-like nanostructures of $SrSnO_3$ showed high photocatalytic activity for hydrogen evolution from a methanol-water solution [21]. All these results suggest that it is possible to synthesize photocatalysts with unique morphologies by this simple and efficient method.

A layered perovskite compound, $Sr_2Ta_2O_7$, has been studied as a well known ferroelectric material. The structure of $Sr_2Ta_2O_7$ is composed of perovskite-type slabs with a thickness corresponding to twice the face diagonal of a perovskite cube. The slabs consist of TaO_6 octahedra connected by sharing corners[22]. Recently, it has been found that $Sr_2Ta_2O_7$ prepared by the SSR method are highly active photocatalyst for water splitting into H_2 and O_2[23,24]. However, to the best of our knowledge, there has been no report on the photocatalytic activity of hydrothermally synthesized $Sr_2Ta_2O_7$ nanosheets for degradation of pollutant contaminates. Here, we report the photocatalytic activities of $Sr_2Ta_2O_7$ nanosheets obtained via a hydrothermal route for the decomposition of methyl orange under UV light irradiation, and the result shows that the activity of the title nanosheets is distinctly more active than that of SSR $Sr_2Ta_2O_7$.

1 Experimental

1.1 Synthesis

$Sr_2Ta_2O_7$ photocatalyst was prepared through a hydrothermal process as previously reported by us[25]. The typical synthesis procedure was as follows: 2.5 g of $Sr(NO_3)_2 \cdot 4H_2O$ and 0.36 g of NaOH were dissolved in deionized water (10 mL), to which 0.65 g of Ta_2O_5 powder was then added under stirring. After stirring for 2 h at room temperature, the resulting slurry was loaded into a 15 mL Teflon stainless autoclave (~80% fill). Then the Teflon stainless autoclave was sealed and maintained at 260 ℃ for 7 d under autogenerated pressure. After natural cooling, the as-obtained products were filtered off, washed with deionized water, and finally dried at 80 ℃ for 5 h. For comparison, the bulk $Sr_2Ta_2O_7$ sample (SSR $Sr_2Ta_2O_7$) was also prepared by the conventional SSR method according to the literature[23].

1.2 Characterization

The crystal structures of the obtained materials were confirmed by a powder X-ray diffractometer (XRD, Rigaku D/max-2000) with monochromated Cu $K\alpha$ radiation (λ=0.154 18 nm, 45 kV, 50 mA). The samples were scanned from 10° to 80° (2θ). Ultraviolet-visible (UV-Vis) diffuse reflectance spectra were recorded for the catalysts using a UV-Vis spectrometer with an intergrating sphere (PG, TU-1900). Surface areas were determined by low temperature nitrogen adsorption-desorption measurement (BF, ST2000). Morphologies were observed by scanning electron microscopy (SEM, Hitachi, S-4800, 15 kV) and transmission electron microscopy (TEM, FEI, Tecnai G2 S-Twin, 200 kV).

1.3 Photocatalytic activities

The photocatalytic activities of $Sr_2Ta_2O_7$ photocatalyst were evaluated by the decomposition of methyl orange under UV light irradiation. A 350W high pressure Hg lamp with a maximum emission at 365 nm

was used as the light source. Aqueous suspension of methyl orange(10 mg·L^{-1}, 100 mL) and 100 mg of the powder was placed in a quartz vessel. Prior to irradiation, the suspension was first ultrasonicated for 10 min, and then magnetically stirred in the dark for 30 min to ensure adsorption equilibrium. The suspension was kept under constant air-equilibrated conditions before and during the irradiation. pH value of the reaction suspension was not adjusted. At given time intervals, 3 mL aliquots were sampled, and centrifugated to remove the particles. The filtrates were analyzed by recording the variations of the absorption band maximum(464 nm) in UV-Vis spectra of the dyes using a PG, TU-1901 spectrometer. The cycling experiment was carried out for testing the lifetime of the obtained photocatalyst. In the present work, five cycling runs were used. At the end of each run, the suspension was filtered off and washed with deionized water for several times, then 100 mL(10 mg·L^{-1}) methyl orange solution was added and tested again under the same measurement conditions.

2　Results and discussion

2.1　Synthesis of $Sr_2Ta_2O_7$ nanosheets

Fig.1 shows the XRD pattern of $Sr_2Ta_2O_7$ nanosheets synthesized at 260 ℃ for 7 d in the presence of 0.8 mol·L^{-1} NaOH solutions. All diffraction peaks can be readily assigned to a pure phase $Sr_2Ta_2O_7$(PDF No.30-1304) and no diffraction peaks from impurity phase were observed. The XRD diffraction pattern indicates that $Sr_2Ta_2O_7$ has a layered pyrochlore crystal structure, space group Cmcm.

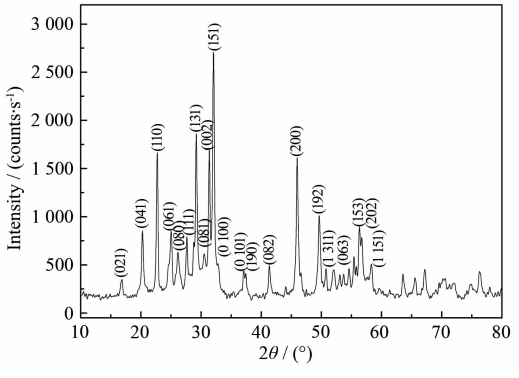

Fig.1　XRD pattern of $Sr_2Ta_2O_7$ nanosheet obtained by a hydrothermal method

2.2　Morphology and photoabsorbance property of $Sr_2Ta_2O_7$ nanosheets

Fig.2 presents the SEM and TEM images of the $Sr_2Ta_2O_7$ nanosheets. It is notable that large-scale amount of $Sr_2Ta_2O_7$ nanosheets are obtained through the hydrothermal process, as shown in Fig.2a. The TEM image further demonstrates the formation of $Sr_2Ta_2O_7$ nanosheets. Fig.2b indicates that the $Sr_2Ta_2O_7$ nanosheets display a regularly shaped morphology. The inset in Fig.2b shows the selected area electron diffraction (SAED) pattern of the $Sr_2Ta_2O_7$ nanosheet. The SAED pattern of a random $Sr_2Ta_2O_7$ nanosheet indicates that these nanosheets are single crystal in nature.

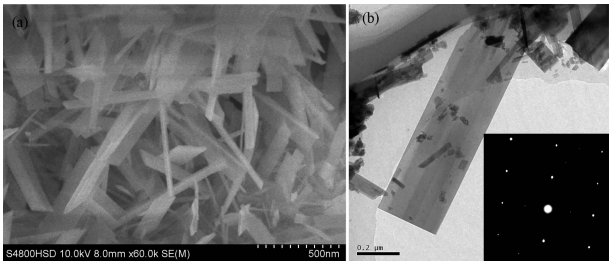

Fig.2　(a) SEM image and (b)TEM image of $Sr_2Ta_2O_7$ nanosheets, the inset in (b) is the SAED pattern of $Sr_2Ta_2O_7$ nanosheets

The UV-Vis diffuse reflectance spectrum of $Sr_2Ta_2O_7$ is given in Fig.3. For a crystalline semiconductor, the optical absorption near the band edge follows the equation $ah\nu=A(h\nu-E_g)^{n/2}$, where a, ν, E_g, and A are absorption coefficient, light frequency, band gap, and a constant, respectively[26]. Because the $Sr_2Ta_2O_7$ is a direct semiconductor, the value of n for $Sr_2Ta_2O_7$ is 1. The band gap of $Sr_2Ta_2O_7$ is estimated to be 4.6 eV from the onset of the absorption edge.

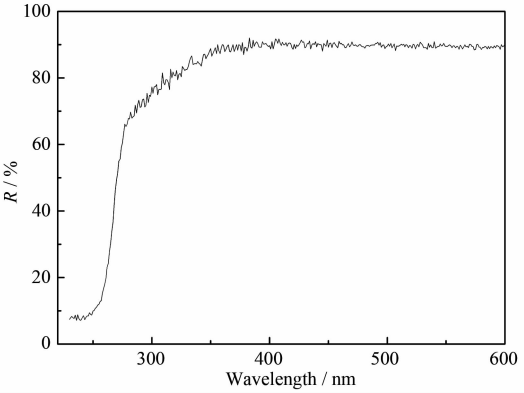

Fig.3　Diffuse reflectance spectra of $Sr_2Ta_2O_7$ nanosheets

Therefore, the catalyst only has absorption in the UV region. The color of $Sr_2Ta_2O_7$ sample is white, as can be expected from the absorption spectrum.

2.3 Photocatalytic performance

Fig.4 gives the decolorization of methyl orange solution upon the addition of $Sr_2Ta_2O_7$ nanosheets under UV light. It is worthy to note that the absorption of methyl orange at 464 nm gradually decreases with the extention of the irradiation time when the mixed solution of methyl orange and $Sr_2Ta_2O_7$ nanosheets is exposed to UV irradiation from high-pressure mercury lamp at room temperature, and the methyl orange solution is almost decolorized when the irradiated time is up to 40 min.

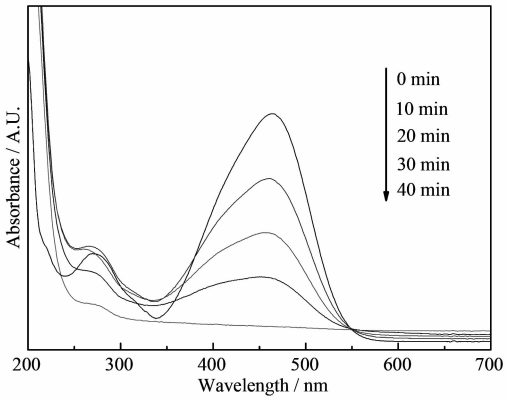

Fig.4 Degradation curves of methyl orange solutions irradiated under ultraviolet light for different time

The high activity of $Sr_2Ta_2O_7$ can also be confirmed from Fig.5. Firstly, The dark experiment demonstrates that the decolorizing efficiency is almost zero(that is to say, the initial methyl orange solution remains unchanged) in the presence of 0.1 g $Sr_2Ta_2O_7$ nanosheets in the dark for 40 min as shown in Fig.5a. The blank test (Fig.5b) confirms that methyl orange can only be slightly degraded under UV light without catalyst, suggesting that the photolysis and adsorption of catalysts can be ignored. Hence, it is inferred that the degradation of methyl orange is dominatingly a photocatalytic process, and $Sr_2Ta_2O_7$ nanosheets can efficiently promote this process. For comparison, the photocatalytic activity of the bulk $Sr_2Ta_2O_7$ sample obtained by the SSR method was also conducted in the present system, as shown in Fig.5c. It can be seen that

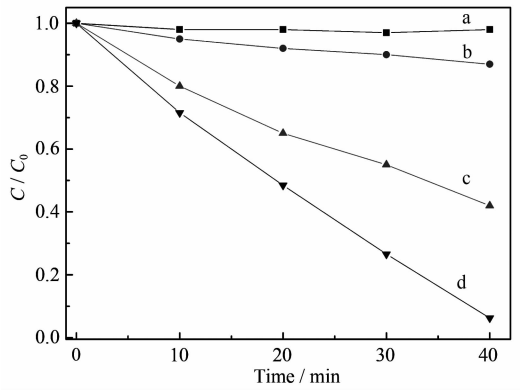

(a) a dark experiment (without irradiation); (b) a blank experiment(in the absence of $Sr_2Ta_2O_7$); (c) bulk $Sr_2Ta_2O_7$ sample under irradiation; and (d) $Sr_2Ta_2O_7$ nanosheets under irradiation

Fig.5 Degradation rate(C/C_0) of methyl orange as a function of irradiation time(C_0 and C were the equilibrium concentration of methyl orange before and after UV irradiation, respectively)

the photocatalytic activity of the bulk $Sr_2Ta_2O_7$ sample for degradation of methyl orange is found to be less active compared to the $Sr_2Ta_2O_7$ nanosheets(Fig.5d). It is known that the surface area of a semiconductor is one of the important factors to determine the activity of a photocatalyst. The BET surface area of $Sr_2Ta_2O_7$ nanosheet is 30 $m^2 \cdot g^{-1}$, 30 times larger than that of the bulk $Sr_2Ta_2O_7$ sample(1 $m^2 \cdot g^{-1}$)[23] The large difference in the surface area results in the different photocatalytic activities. The results further confirm that the hydrothermal method is a simple and efficient approach to obtain photocatalyts with high activity.

The lifetime for $Sr_2Ta_2O_7$ nanosheets is shown in Fig.6, after five recycles for the degradation of methyl orange, no obvious loss of activity is observed, indicating that $Sr_2Ta_2O_7$ nanosheets are not deactivated during the photocatalytic oxidation of the pollutant molecules. Fig.7 shows the XRD patterns of the $Sr_2Ta_2O_7$ catalyst before and after photocatalytic reaction. No structural difference between the samples before and after reaction is observed, further confirming that $Sr_2Ta_2O_7$ nanosheets function as the photocatalyst in the process of decolorization. Fu et al[3] suggested that the catalyst crystallized in the water medium of the hydrothermal condition showed stable activity for photodegradation of organic pollutants, because the hydrothermal process can allow the crystallization of

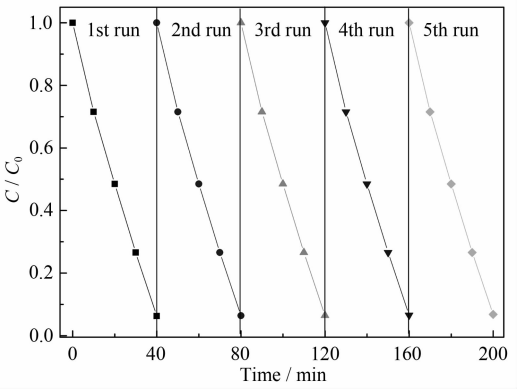

Fig.6　Cycling runs in the photocatalytic degradation of methyl orange in the presence of $Sr_2Ta_2O_7$ nanosheets under UV irradiation

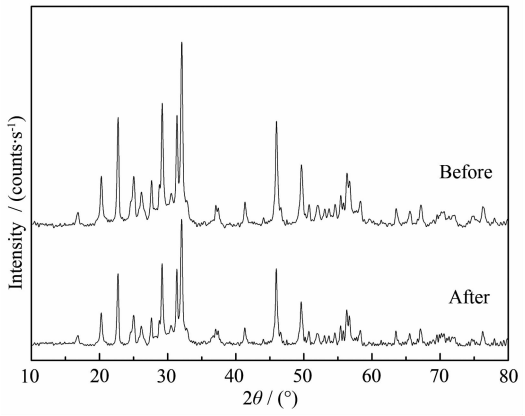

Fig.7　XRD patterns of $Sr_2Ta_2O_7$ nanosheets before and after photocatalytic reaction.

the catalyst under mild conditions for a long period of time.

3　Conclusions

$Sr_2Ta_2O_7$ cat alyst was synthesized by a simple hydrothermal process and its photocatalytic activity was evaluated by degradation of methyl orange. The result suggests that the $Sr_2Ta_2O_7$ nanosheets prepared by the hydrothermal method show a much higher degradation efficiency for methyl orange under ultraviolet light irradiation than the bulk $Sr_2Ta_2O_7$ sample obtained by the SSR method. The results also indicate that the hydrothermal method would be helpful in exploiting the complex oxide photocatalysts.

References:

[1] Fujishima A, Hond K. *Nature*, **1972**,**238**:37~38

[2] Zou Z G, Ye J H, Arakawa H. *Nature*, **2001**,**414**:625~627

[3] Fu H B, Lin J, Zhang L W, et al. *Appl. Catal. A*, **2006**,**306**: 58~67

[4] Li J, Ni Y H, Liao K M, et al. *J. Colloid Interf. Sci.*, **2009**, **332**:231~236

[5] Chen Z X, Li D Z, Zhang W J, et al. *J. Phys. Chem. C*, **2009**, **113**:4433~4440

[6] YANG Ya-Hui(杨亚辉), CHEN Qi-Yuan(陈启元), LI Jie (李　洁), et al. *Chinese J. Inorg. Chem.* (*Wuji Huaxue Xuebao*), **2009**,**25**:256~263

[7] Lin X P, Huang F Q, Wang W D, et al. *Appl. Catal. A*, **2006**, **307**:257~262

[8] Zhang L W, Fu H B, Zhang C, et al. *J. Phys. Chem. C*, **2008**, **112**:3126~3133

[9] Yu J G, Yu X X. *Environ. Sci. Technol.*, **2008**,**42**:4902~4907

[10]Li X K, Ouyang S, Kikugawa N, et al. *Appl. Catal. A.*, **2008**, **334**:51~55

[11]Du W M, Zhu J, Li S X, et al. *Cryst. Growth Des.*, **2008**,**8**: 2130~2136

[12]Zhou L, Wang W Z, Xu H L, et al. *Cryst. Growth Des.* **2008**, **8**:3595~3601

[13]Tang J W, Zou Z G, Ye J H. *J. Phys. Chem. C*, **2007**,**111**: 12779~12785

[14]SHEN Jing-Jing(沈晶晶), LIU Chang(刘　畅), ZHU Yu-Dan (朱育丹), et al. *Acta Phys. -Chim. Sin.* (*Wuli Huaxue Xuebao*), **2009**,**25**:1013~1018

[15]Xu TG, Zhang C, Shao X, et al. *Adv. Funct. Mater.*, **2006**, **16**:1599~1607

[16]Zeng J, Wang H, Zhang Y C, et al. *J. Phys. Chem. C*, **2007**, **111**:11879~11887

[17]Cho I S, Lee S, Noh J H, et al. *J. Phys. Chem. C*, **2008**,**112**: 18393~18398

[18]BAO Nan (包　南), SUN Jian (孙　剑), ZHANG Feng (张　锋), et al. *Chinese J. Inorg. Chem.* (*Wuji Huaxue Xuebao*), **2007**,**23**:101~108

[19]Fu H B, Pan C S, Yao W Q, et al. *J. Phys. Chem. B*, **2005**, **109**:22432~22436

[20]Cao F, Shi W D, Zhao L J, et al. *J. Phys. Chem. C*, **2008**, **112**:17095~17101

[21]Chen D, Ye J H. *Chem. Mater.*, **2007**,**19**:4585~4591

[22]Ishizawa N, Marumo F, Kawamura T. *Acta Cryst. B*, **1976**, **32**:2564~2566

[23]Kudo A, Kato H, Nakagawa S. *J. Phys. Chem. B*, **2000**,**104**: 571~575

[24]Kato H, Kudo A. *J. Photochem.Photobio. A*: *Chem.*, **2001**, **145**:129~133

[25]Zhou C, Chen G, Li Y X, et al. *Int. J. Hydrogen Energy*, **2009**,**34**:2113~2120

[26]Butler M A. *J. Appl. Phys.*, **1977**,**48**:1914~1918